*Ultrasound Obstet Gynecol* 2015
Published online in Wiley Online Library (wileyonlinelibrary.com). **DOI:** 10.1002/uog.14806

# Terms, definitions and measurements to describe sonographic features of myometrium and uterine masses: a consensus opinion from the Morphological Uterus Sonographic Assessment (MUSA) group

T. VAN DEN BOSCH*#, M. DUEHOLM†#, F. P. G. LEONE‡, L. VALENTIN§, C. K. RASMUSSEN†, A. VOTINO¶, D. VAN SCHOUBROECK*, C. LANDOLFO**, A. J. F. INSTALLÉ†††‡‡, S. GUERRIERO§§, C. EXACOUSTOS¶¶, S. GORDTS***, B. BENACERRAF†††, T. D'HOOGHE‡‡‡, B. DE MOOR†††‡‡, H. BRÖLMANN§§§, S. GOLDSTEIN¶¶¶, E. EPSTEIN^, T. BOURNE*~ and D. TIMMERMAN*

**Department of Obstetrics and Gynecology, University Hospitals KU Leuven, Leuven, Belgium; †Department of Obstetrics and Gynecology, Aarhus University Hospital, Aarhus, Denmark; ‡Department of Obstetrics and Gynecology, Clinical Sciences Institute L Sacco, University of Milan, Milan, Italy; §Department of Obstetrics and Gynecology, Skåne University Hospital, Lund University, Malmö, Sweden; ¶Department of Obstetrics and Gynecology, Brugmann University Hospital, Brussels, Belgium; **Department of Obstetrics and Gynecology, Sant' Orsola-Malpighi Hospital, University of Bologna, Bologna, Italy; ††KU Leuven, Department of Electrical Engineering (ESAT), STADIUS, Center for Dynamical Systems, Signal Processing and Data Analytics, Leuven, Belgium; ‡‡iMinds Medical IT, Leuven, Belgium; §§Department of Obstetrics and Gynaecology, Azienda Ospedaliera Universitaria of Cagliari and University of Cagliari, Cagliari, Italy; ¶¶Department of Biomedicine and Prevention, Obstetrics and Gynecological Clinic, University of Rome 'Tor Vergata', Rome, Italy; ***L.I.F.E. (Leuven Institute for Fertility & Embryology), Leuven, Belgium; †††Departments of Radiology and Obstetrics & Gynecology, Harvard Medical School, Boston, MA, USA; ‡‡‡Leuven University Fertility Centre, University Hospitals KU Leuven, Leuven, Belgium; §§§Department of Obstetrics and Gynecology, VU University Medical Center, Amsterdam, The Netherlands; ¶¶¶Department of Obstetrics and Gynecology, New York University School of Medicine, New York, NY, USA; ^Department of Obstetrics and Gynecology, Karolinska University Hospital, Stockholm, Sweden; ~Queen Charlotte's and Chelsea Hospital, Imperial College, London, UK*

**KEYWORDS:** adenomyosis; consensus; fibroids; leiomyosarcoma; myometrium; ultrasonography; uterus

## ABSTRACT

*The MUSA (Morphological Uterus Sonographic Assessment) statement is a consensus statement on terms, definitions and measurements that may be used to describe and report the sonographic features of the myometrium using gray-scale sonography, color/power Doppler and three-dimensional ultrasound imaging. The terms and definitions described may form the basis for prospective studies to predict the risk of different myometrial pathologies, based on their ultrasound appearance, and thus should be relevant for the clinician in daily practice and for clinical research. The sonographic features and use of terminology for describing the two most common myometrial lesions (fibroids and adenomyosis) and uterine smooth muscle tumors are presented. Copyright © 2015 ISUOG. Published by John Wiley & Sons Ltd.*

## INTRODUCTION

Ultrasonography is a first-stage imaging technique for assessing the myometrium and requires findings to be reported consistently. Recently, the International Federation of Gynecology and Obstetrics (FIGO) PALM-COEIN system (polyp; adenomyosis; leiomyoma; malignancy and hyperplasia; coagulopathy; ovulatory dysfunction; endometrial; iatrogenic; not yet classified)[1,2] was published, which classifies the etiology of abnormal uterine bleeding, including the myometrial pathologies adenomyosis and fibroids. However, implementation of this classification system in daily clinical practice is hampered by the lack of standardization of the terms and definitions used to describe ultrasound findings. Standardized terms to be used when describing ultrasound images of the endometrium and uterine cavity have been suggested by the IETA (International Endometrial Tumor Analysis) group[3], but there remains no standardized terminology for describing ultrasound images of normal or pathological myometrium, or uterine masses[4].

In clinical practice and research, standardized reporting of ultrasound findings, with regard to the myometrium, is essential to reduce intra- and interobserver variability in the evaluation of pathology, to assess the effect of medical or surgical treatment and to compare ultrasound

*Correspondence to:* Dr T. Van den Bosch, Department of Obstetrics and Gynecology, University Hospitals KU Leuven, Herestraat 49, 3000 Leuven, Belgium (e-mail: thierryvandenbosch1901@gmail.com)

#T.V.d.B. and M.D. are joint first authors.

*Accepted: 27 January 2015*

imaging with other imaging techniques. Moreover, common terminology is necessary for comparison of studies and when combining data in meta-analyses. Reliable predictors of benign pathology are essential clinically to allow safe use of minimally invasive techniques, such as selective uterine artery embolization, fibroid ablation or laparoscopic morcellation[5], for the treatment of uterine myomas.

The primary aim of this paper was to present a consensus opinion on the terminology to be used when describing the ultrasonographic features of the myometrium and myometrial lesions. These terms and definitions should be relevant both for clinicians reporting ultrasound examinations in day-to-day practice and for clinical research. A secondary aim was to illustrate use of the terminology when describing the two most common myometrial lesions: fibroids and adenomyosis.

This Morphological Uterus Sonographic Assessment (MUSA) consensus paper is based on the opinion of a panel of clinicians with expertise that includes gynecological ultrasonography, fertility treatment, hysteroscopy, general gynecology and clinical research. Amongst the authors were members from the IOTA (International Ovarian Tumor Analysis) and IETA groups and, in order to produce a consensus paper that includes opinions from both ultrasound and endoscopic interest groups, members of the ESGE (European Society of Gynaecological Endoscopy) were also included.

## EXAMINATION OF THE MYOMETRIUM

Ultrasound examination of the myometrium may be performed using a transabdominal (TAS) or transvaginal (TVS) approach. Although examination by high-resolution TVS is preferred generally, allowing for detailed assessment of the myometrium within a limited depth of view, TAS may be necessary for imaging beyond the small pelvis. For adequate visualization of the uterus, some bladder filling will be required to displace the small bowel from the field of view. Image quality during TAS may be hampered by adiposity, scar tissue or uterine retroversion. Examination by TVS commences with a dynamic two-dimensional (2D) scan of the uterus in two perpendicular planes. Some gentle pressure applied by either the probe or the examiner's free hand may be required to assess uterine mobility and to screen for site-specific tenderness[6].

On a sonographic cross-section through the uterus, the arcuate venous and arterial vessels can be seen in close proximity to the outer myometrial border. The junctional zone (JZ) (also referred to as inner myometrium, archimyometrium or stratum subvasculare) is visible as a hypoechogenic subendometrial halo. This layer is composed of longitudinal and circular closely packed smooth-muscle fibers[7].

Three-dimensional (3D) ultrasonography enables the offline examination and manipulation of ultrasound images. In difficult cases this may facilitate access to a second opinion from an expert examiner. To acquire the 3D volume of the uterus, an adequately enlarged midsagittal or transverse section of the uterine body is obtained. In optimal conditions, the midsagittal plane allows visualization of the entire length of the endometrium as well as the endocervical canal. The acquisition angle chosen should include the entire uterine volume of interest. Once the 3D volume has been acquired, its examination is performed in the multiplanar view by scrolling in each sectional plane separately.

Coronal sections of the uterus provide information on the external uterine contour and cavity shape.

Different features for image optimization and postprocessing are used. For example, rendering and volume contrast imaging (VCI) modes provide details on the continuity and thickness of the JZ[8–10]. Other postprocessing modalities, such as TUI (also called multislice imaging), may also be helpful.

### Uterine measurement, shape and external contour

The uterine corpus is measured as shown in Figure S1. If the purpose of the ultrasound scan is to evaluate the myometrium (e.g. in the diagnosis of adenomyosis), then measurement of the uterine volume should exclude the cervix. If the length of the entire uterus (including the cervix) is required (e.g. at preoperative evaluation), the sum of the total length of the uterine corpus (d1) and the cervical length should be reported. d1 is calculated as the sum of the fundal length (from the fundal serosal surface of the uterus to the fundal tip of the endometrial cavity) and the endometrial cavity length (from the fundal tip of the endometrial cavity to the internal os of the cervix). Preferentially, each should be measured separately in the longitudinal plane of the uterus. The longest anteroposterior diameter (d2) of the uterus is measured in the sagittal plane and the longest transverse diameter is measured in the transverse plane. The formula for uterine volume calculation based on these measurements is displayed in Table 1 and Figure S1. The serosal contour of the uterus is reported as either regular or lobulated (Figure S2).

The anterior and posterior myometrial walls are measured from the external uterine serosa to the external endometrial contour and should include the JZ but not the endometrium. The myometrial walls are measured in the sagittal plane, perpendicular to the endometrium. Both measurements are recorded from the same image, and the measurements should be obtained from the thickest point of the myometrial wall. The ratio between the anterior and posterior wall thickness is calculated. A ratio of around 1 indicates that the myometrial walls are symmetrical and a ratio well above or below 1 indicates asymmetry, although this may also be estimated subjectively (Figure S3). The myometrial walls can also be measured in the transverse or coronal planes if deemed necessary.

### The junctional zone (JZ)

Although the JZ can often be visualized on 2D ultrasound, acquisition of a 3D volume enables a more complete assessment in the sagittal, transverse and coronal planes,

 

**Table 1** Reporting the myometrium on ultrasound examination

| *Feature* | *Description/term* | *Quantification/measurement* |
|---|---|---|
| Uterine corpus*† (Figure S1) | Length, anteroposterior diameter, transverse diameter, volume* | Length (d1) = [fundus] + [cavity]; anteroposterior diameter (d2); transverse diameter (d3); volume ($cm^3$) = d1 (cm) × d2 (cm) × d3 (cm) × 0.523† |
| Uterine corpus and cervix† (Figure S1) | — | Total length = [fundus] + [cavity] + [cervix] = d1 + c† |
| Serosal contour† (Figure S2) | Regular/lobulated† | — |
| Myometrium | | |
| Myometrial walls* (Figure S3) | Symmetrical/asymmetrical* | Ratio or subjective impression of asymmetry* |
| Overall echogenicity* | Homogeneous/heterogeneous* | — |
| Myometrial lesions* | Well-defined/ill-defined* | — |
| Number* | — | Exact number (*n*)* |
| Location*‡ | Location: anterior, posterior, fundal, right lateral or left lateral, global* | — |
| Site (Figure 3)*‡ | Site (for well-defined lesions): FIGO-classification 1–7* | — |
| Size*†‡ | — | Three perpendicular diameters (a1, a2, a3) and/or volume ($cm^3$) = a1 (cm) × a2 (cm) × a3 (cm) × 0.523† |
| Outer lesion-free margin (OFM)†‡ (Figure S5) | — | Minimum distance between serosal surface and outermost border of lesion†‡ |
| Inner lesion-free margin (IFM)†‡ (Figure S5) | — | Minimum distance between endometrium and inner border of lesion†‡ |
| Penetration of ill-defined lesions† (Figure S6) | Ratio between thickness of lesion and the total uterine wall thickness, measured on the same image† | Penetration = maximum diameter of lesion perpendicular to endometrium/maximum wall thickness perpendicular to endometrium† |
| Extent of ill-defined lesions† | Localized (< 50% of total uterine volume involved) or diffuse (≥ 50% of total uterine volume involved)† | Proportion (%) of myometrium volume involved† |
| Echogenicity† (Figures 4 and S7) | Uniform: hypo-, iso-, hyper-echogenic; non-uniform: mixed echogenicity, cystic areas (regular/irregular); anechogenic, low level, ground glass, mixed echogenicity of cyst fluid† | Very hypoechogenic (– –), hypoechogenic (–), isoechogenic, hyperechogenic (+), very hyperechogenic (++)† |
| Rim† (Figure S8) | Hypo- or hyperechogenic, or ill-defined† | — |
| Shape† (Figure S8) | Round/not-round: oval, lobulated, irregular† | — |
| Shadowing (Figure 5a) | | |
| Edge*† | Present/absent* | Degree of shadowing: slight, moderate, strong† |
| Internal*† | Present/absent* | Degree of shadowing: slight, moderate, strong† |
| Fan-shaped*† (Figure 5c) | Present/absent* | Degree of shadowing: slight, moderate, strong† |
| Cysts* (Figure 6a) | Present/absent* | — |
| Size† | — | Maximum diameter of largest cyst† |
| Number of cysts† | — | Exact number (or single, 1–5, > 5) † |
| Echogenicity† | Cyst fluid: anechogenic, low level, ground glass, mixed echogenicity; hyperechogenic rim: present/absent† | — |
| Hyperechogenic islands* (Figure 6b) | Present/absent* | — |
| Outline† | Regular, irregular or ill-defined† | — |
| Size† | — | Maximum diameter† |
| Number† | — | Exact number (or single, 1–5, > 5)† |
| Subendometrial echogenic lines and buds* (Figure 7) | Present/absent* | — |
| Number† | — | Exact number (or single, 1–5, > 5) |
| | | Location† |

Definitions of terms and their quantifications are described in text and illustrated by ultrasound images and schematic diagrams. Measurements are reported in mm or cm (to tenths of a cm). *Items of importance in daily clinical practice. †Items of interest for research purposes. ‡If clinically relevant (e.g. preoperative work-up before myomectomy).

 

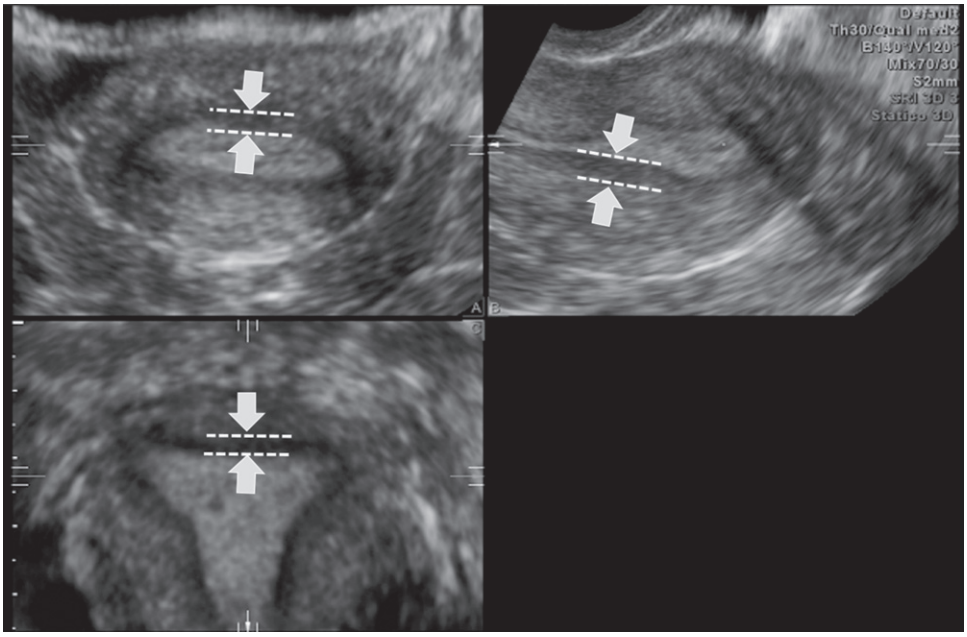

**Figure 1** Multiplanar view of the uterine corpus obtained by three-dimensional ultrasound. The junctional zone (JZ) can be seen as a dark line just beneath the endometrium (arrows and dashed lines). The JZ of the anterior and posterior wall is visualized in the A- and B-planes and the JZ of the left and right lateral walls and of the fundus in the C-plane.

**Table 2** Reporting the junctional zone (JZ) on ultrasound examination

| *Structure* | *Description* | *Measurement* |
|---|---|---|
| JZ*† | Regular, irregular, interrupted, not visible, not assessable* | Maximum ($JZ_{max}$) and minimum ($JZ_{min}$) JZ thickness in mm or ratio JZ/total myometrial wall thickness† |
| Irregular or interrupted JZ† | Location: anterior, posterior, fundus, lateral right, lateral left, or global† | Magnitude of irregularity: $(JZ_{max}) - (JZ_{min}) = JZ_{dif}$; extent of irregularity: proportion (%) of JZ that is irregular ($< 50\%$ or $\geq 50\%$)† |
| Interrupted JZ† | Location: anterior, posterior, fundus, lateral right, lateral left, or global† | Interruption of JZ: proportion (%) of JZ not visualized ($< 50\%$ or $\geq 50\%$)† |
| Irregularity in JZ† | Cystic areas, hyperechogenic dots, hyperechogenic buds and lines (in each location)† | — |

Definitions of terms and their quantifications are described in text and illustrated by ultrasound images and schematic diagrams (Figures 2 and S4). *Items of importance in daily clinical practice. †Items of interest for research purposes.

as shown in a standardized multiplanar view[11] (Figure 1). Using the standardized multiplanar view reduces interobserver variation in measurements, is used in general clinical practice for evaluation of the coronal view[12] and may be obtained by the z-rotation technique[13]. Imaging of the JZ may be optimized by using a postprocessing rendering mode, for example VCI. The thickness of the slices or render box may be selected from between 1 mm and 4 mm[9].

The JZ (Table 2 and Figure 2) may be reported as regular, irregular, interrupted, not visible or not assessable[3] or may manifest more than one feature (e.g. irregular and interrupted). For research purposes, any irregularity in the JZ may be described (e.g. cystic areas, hyperechogenic dots, hyperechogenic buds and lines) in each location (anterior, posterior, lateral left, lateral right, fundus) according to the specific research protocol. Detailed morphological assessment and measurement of the JZ is generally relevant only in the context of research protocols. The JZ and the total uterine wall thickness are measured perpendicular to the endometrium on the same section through the uterus. The maximum thickness of the JZ ($JZ_{max}$) is measured at the area in which it appears to be thickest, and the minimum thickness ($JZ_{min}$) is measured where it appears to be thinnest, after evaluation of the total 3D volume of the uterus (Figure S4). To define the ratio between the JZ and the total uterine wall thickness, both measurements should be recorded from the same image. From where the measurement(s) should be taken to calculate this ratio depends on the research protocol. If the JZ is ill-defined or not visible, it should be reported as 'non-measurable'.

The magnitude and extent of any irregularity of the JZ may be reported and its JZ location (anterior, posterior, lateral left, lateral right, fundus) specified according to the research protocol. The magnitude of a JZ irregularity is expressed as the difference between the maximum and minimum JZ thickness: $(JZ_{dif}) = JZ_{max} - JZ_{min}$. The extent of the irregularity is reported as the subjective

 

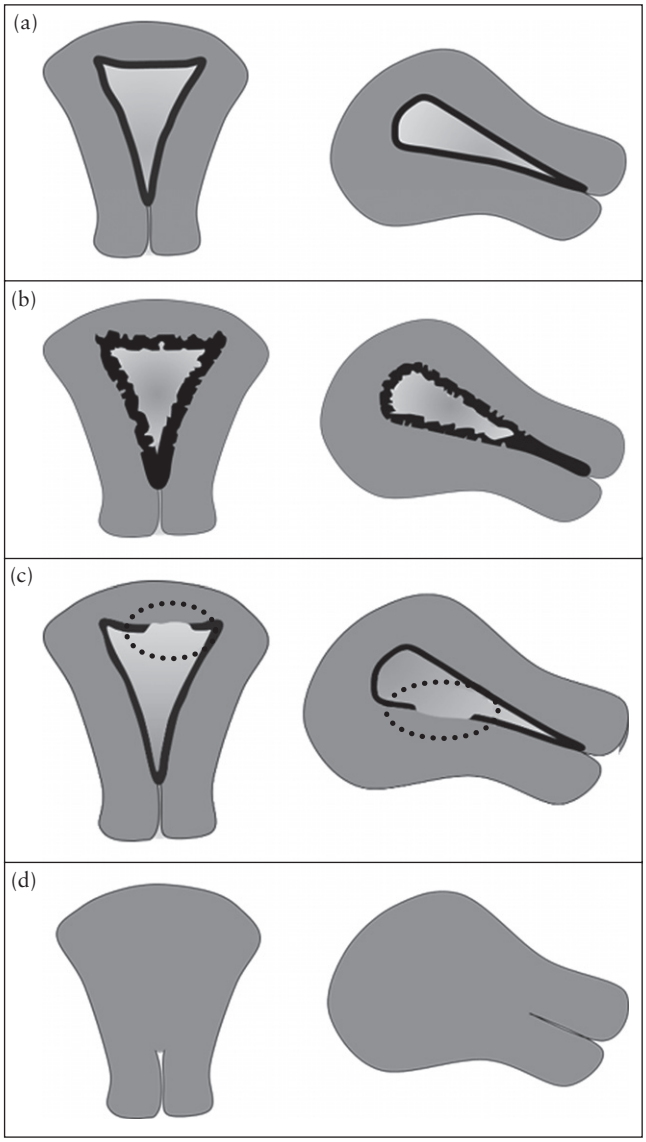


**Figure 2** Schematic drawings illustrating a regular (a), irregular (b), interrupted (c) and not visible (d) junctional zone displayed in the coronal plane (left) and in the sagittal plane (right).

estimation of the percentage of the JZ that is irregular ($< 50\%$ or $\geq 50\%$). This estimation can be made for the uterus as a whole or for each location. Interruption of the JZ may be caused by focal infiltration by endometrial tissue, but contractions and changes within the JZ may also give rise to apparent JZ irregularities or influence its thickness. The extent of interruptions is recorded as a subjective estimation of the percentage of the JZ that is interrupted ($< 50\%$ or $\geq 50\%$). Again, this may be calculated for the uterus as a whole or at each specific location.

## Description of myometrial pathology (Table 1)

An evaluation of myometrial pathology includes an assessment of overall myometrial echogenicity, which is reported as homogeneous or heterogeneous. The reason for the heterogeneity (e.g. cysts, shadowing) should be specified as outlined below.

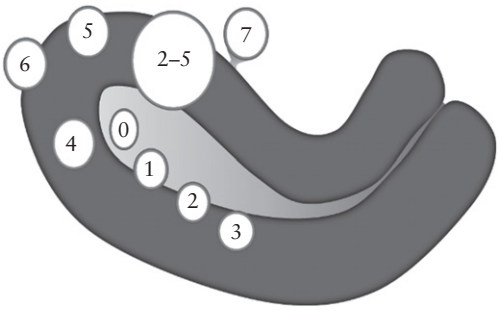


**Figure 3** The FIGO classification of myomas (adapted from Munro *et al.*[2]) should be used to report the site of well-defined localized lesions: 0 = pedunculated intracavitary; 1 = submucosal, $< 50\%$ intramural; 2 = submucosal, $\geq 50\%$ intramural; 3 = 100% intramural, but in contact with the endometrium; 4 = intramural; 5 = subserosal, $\geq 50\%$ intramural; 6 = subserosal, $< 50\%$ intramural; 7 = subserosal pedunculated; 8 = other (e.g. cervical, parasitic)[1,14].

Myometrial pathology may be localized (one or more lesions) or diffuse. A myometrial lesion may be well-defined, as seen typically in fibroids, or ill-defined, as seen typically in adenomyosis. Each lesion should be described according to its location, size and site (Table 1 and Figures 3, S5 and S6), but this may not be possible for some ill-defined lesions. The lesion location within the myometrium may be anterior or posterior, fundal, right lateral or left lateral. A lesion is global if the pathology involves the whole myometrium diffusely. The site of a well-defined lesion should be reported using the FIGO classification for fibroids: 0 = pedunculated intracavitary; 1 = submucosal, $< 50\%$ intramural; 2 = submucosal, $\geq 50\%$ intramural; 3 = 100% intramural, but in contact with the endometrium; 4 = intramural; 5 = subserosal, $\geq 50\%$ intramural; 6 = subserosal, $< 50\%$ intramural; 7 = subserosal pedunculated; 8 = other (e.g. cervical, parasitic)[1,14] (Figure 3). Lesion size is estimated by measuring the three largest orthogonal diameters. The minimum distance from the lesion to the endometrium (inner lesion-free margin) and to the serosal surface (outer lesion-free margin) of the uterus[15,16] is measured as described in Figure S5.

Ill-defined lesions are, by definition, difficult to delineate and measurements may be inaccurate. The extent of an ill-defined lesion can be estimated subjectively as the percentage of the whole myometrial volume that is involved. If $< 50\%$ of the total myometrium is involved, the lesion is reported as localized, if $\geq 50\%$ of the myometrium is involved it is reported as diffuse. For research purposes or in a preoperative setting, the percentage involved in each location may need to be recorded. For ill-defined lesions, the penetration is defined as the ratio between the maximum thickness of the lesion and the total uterine wall thickness. The penetration is measured where the lesion appears to be at its largest, as shown in Figure S6.

The echogenicity of a lesion is reported as uniform (homogeneous and/or having symmetrical pattern of echogenicity) or non-uniform (heterogeneous)

 

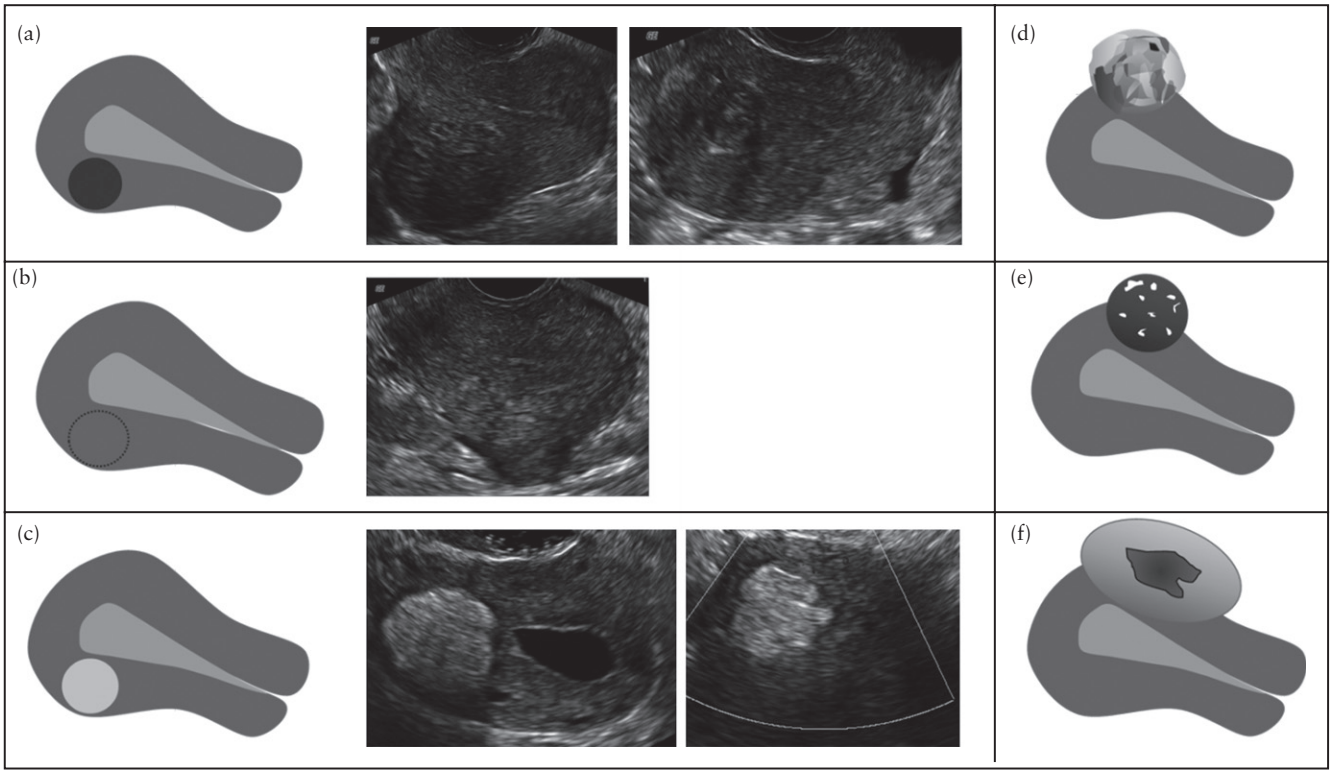


**Figure 4** Schematic drawings and ultrasound images illustrating different types of lesion echogenicity. The echogenicity of a lesion may be uniform (hypoechogenic (a), isoechogenic (b) or hyperechogenic (c)) or non-uniform (with mixed echogenicity (d), echogenic areas (e) or cystic areas (f)).

(Figure 4) and a uniform lesion may be hypo-, iso- or hyperechogenic. For research purposes, the echogenicity of the lesion may be compared to that of the adjacent myometrium and semi-quantified, as shown in Figure S7, as very hypoechogenic (− −), hypoechogenic (−), isoechogenic, hyperechogenic (+) or very hyperechogenic (++). A lesion may have non-uniform echogenicity due to mixed echogenicity or the presence of echogenic areas or cystic areas (regular or irregular). If present, cystic contents may be anechoic, of low-level echogenicity, of ground-glass appearance or of mixed echogenicity[17]. Anechoic areas can be differentiated from large vessels by using power Doppler to confirm the absence of blood flow. The rim of a lesion may be ill-defined, hypoechogenic or hyperechogenic in comparison to the myometrium (Figure S8), and the shape of a lesion may be round or not round. A lesion that is not round may be oval, lobulated or irregular (Figure S8).

Shadowing (Figure 5a) may arise from the edge of a lesion, in which case they are reported as edge shadows, or from areas within the lesion, in which case they are termed internal shadows. The degree of shadowing is reported subjectively as slight, moderate or strong. Fan-shaped shadowing (Figure 5c) is defined by the presence of hypoechogenic linear stripes, sometimes alternating with linear hyperechogenic stripes. This type of shadowing may be caused by overlying (micro)cystic structure(s). The degree of shadowing is recorded subjectively as slight, moderate or strong.

Myometrial cysts (Figure 6a) are rounded lesions within the myometrium. The cystic contents may be anechoic, of low-level echogenicity, of ground-glass appearance or of mixed echogenicity. A cyst may be surrounded by a hyperechogenic rim. In the context of research studies, the number of cysts and the largest diameter of the largest cyst or of a specified number of cysts, as well as the echogenicity of the cystic fluid, may be reported. Some cysts are not measurable individually and may form aggregates of tiny, hypoechogenic microcysts (anechoic lacunae) within the myometrium. There are often several aggregates of microcysts in an area.

Hyperechogenic islands (Figure 6b) are hyperechogenic areas within the myometrium and they may be regular, irregular or ill-defined. The number of hyperechogenic islands and the maximum diameter of the largest (or, if applicable, for example as part of a research protocol, maximum diameter of a specified number of hyperechogenic islands) may be reported. Hyperechogenic islands should be distinguished from small hyperechogenic spots seen in the subendometrium (Figure 6c).

Hyperechogenic subendometrial lines or buds (Figure 7) may be observed disrupting the JZ. Hyperechogenic subendometrial lines are (almost) perpendicular to the endometrial cavity and are in continuum with the endometrium. These buds and lines should be distinguished from small hyperechogenic spots seen in the subendometrium (Figure 6c). For research purposes, the number and location of the subendometrial lines or buds should be reported.

 

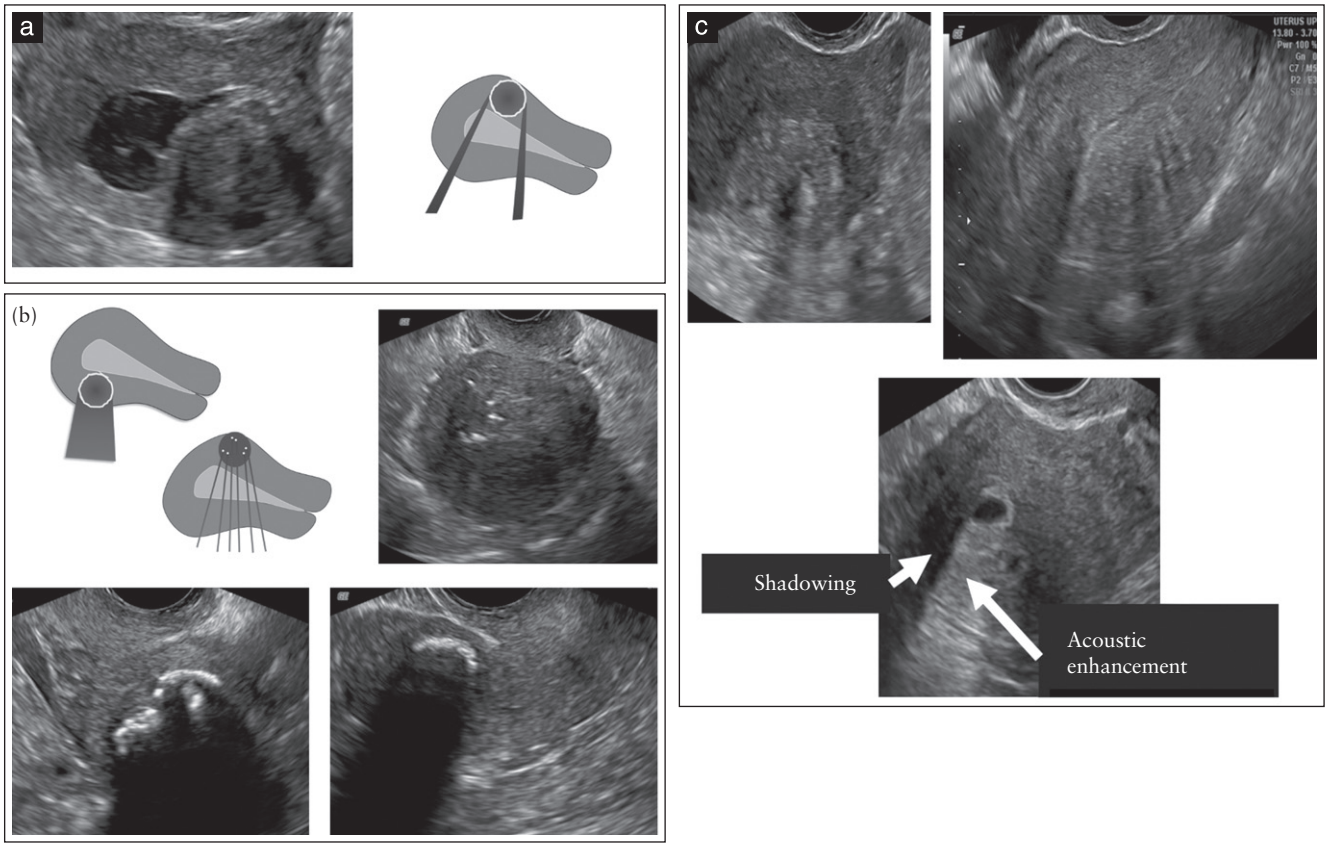


**Figure 5** Schematic diagrams and ultrasound images illustrating edge shadowing (a), internal shadowing (b) and fan-shaped shadowing (c). The lower image in (c) also shows an anechogenic myometrial cyst with a hyperechogenic rim surrounding the cyst and acoustic enhancement posterior to the cyst.

### Vascularization of the myometrium and myometrial lesions

When using color or power Doppler ultrasound, the arcuate vessels of the uterus are often visible at the periphery of the myometrium, running parallel to the uterine serosa. Perpendicular to the arcuate vessels, the radial arteries and veins are usually detectable flowing throughout the myometrium (Figure S9).

The use of power Doppler is preferred to that of color Doppler, because, in general, it is superior for the detection of small vessels with low blood-flow velocities. Color Doppler is used to assess the direction of blood flow. Depending on the area of interest, the color or power Doppler box should include the whole or a specific part of the uterus, or be focused on a myometrial lesion. Magnification and settings should be adjusted to ensure maximum sensitivity, and the Doppler gain should be reduced until all color artifacts disappear. Usually, settings allowing the detection of blood-flow velocities of 3–9 cm/s are optimal, but this may vary from one ultrasound machine to another.

The vascular pattern within the myometrium may be uniform or non-uniform (Figure 8) and the vascular pattern of a myometrial lesion may be circumferential, intralesional or both (Figure 8). Some lesions are associated with disruption of the normal uterine vasculature, while others are not. Translesional vascularity (Figure 9) is characterized by the presence of vessels perpendicular to the uterine cavity/serosa crossing the lesion. The degree of vascularization should be reported using a subjective color score, with a color score of 1 representing no color and a score of 4 representing abundant color signals. This score is based on subjective evaluation of both the percentage of the lesion that is vascularized and the color hue. The color score is assigned taking into account the lesion as a whole, but in lesions with uneven internal vascularization (e.g. because of cystic areas or central necrosis), the score reflects the degree of vascularization in the solid parts of the lesion. If there is an uneven spread of vascularization in the solid components of the lesion, the score for the most vascularized solid component and the percentage of the solid components with color signals should be recorded. A color score may be assigned separately to circumferential and intralesional vascularity (Figure S10).

When carrying out research studies, the vascularity of lesions may be reported as iso-, hypo- or hypervascular compared with the vascularity of the surrounding myometrium. Reporting a lesion's vascularity may include the number of vessels (single or multiple), vessel size (small and equal, large and equal, unequal; or the vessel diameter may be measured), the direction of vessels (perpendicular or not perpendicular to endometrium), the vessel branching pattern (no branching, regular or

 

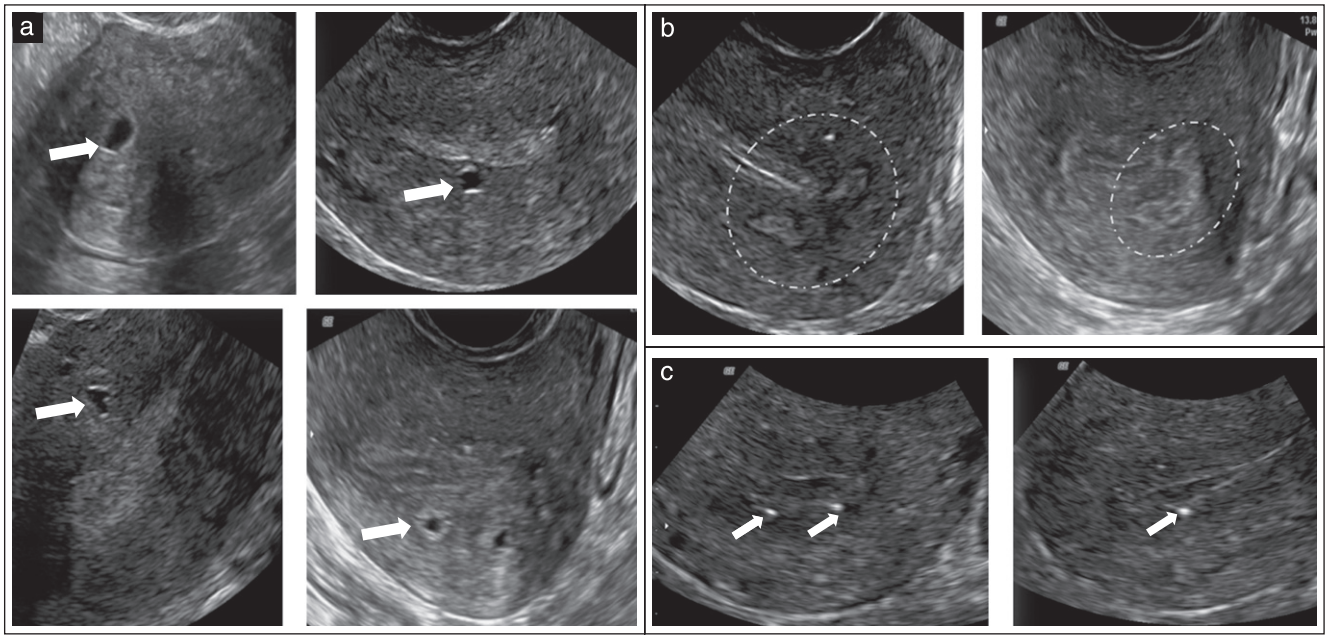


**Figure 6** Ultrasound images showing: (a) myometrial cysts (arrows); (b) hyperechogenic islands (surrounded by dotted lines); and (c) echogenic spots (arrows).

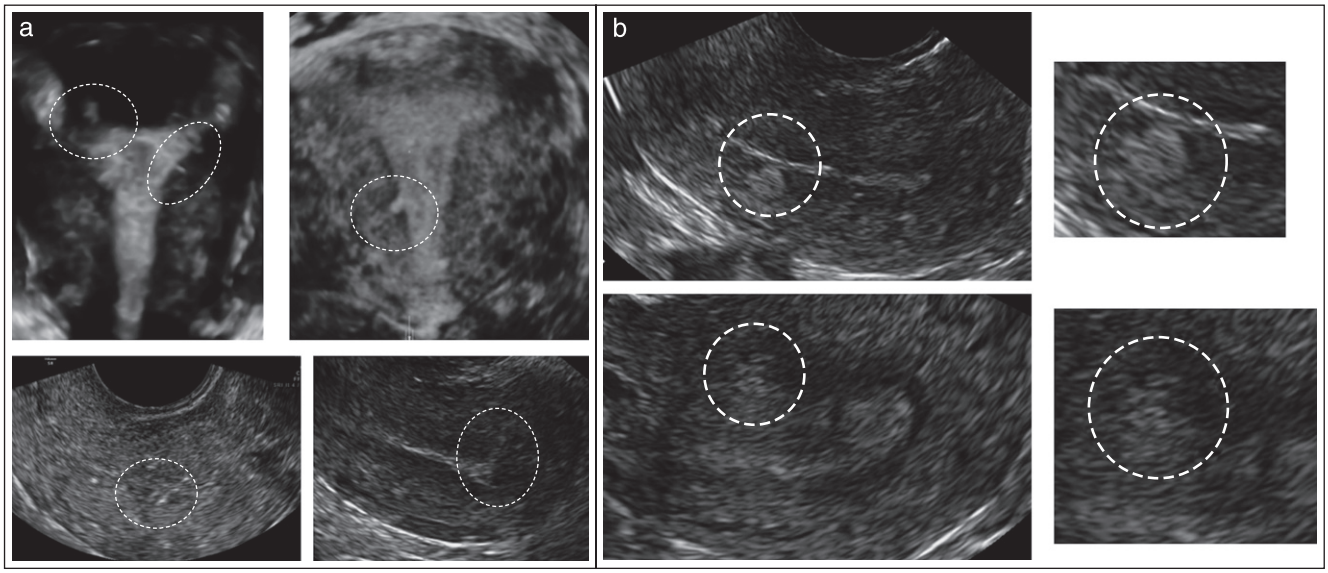


**Figure 7** Ultrasound images illustrating echogenic subendometrial lines (a) and buds (b) (both encircled by dashed lines).

irregular branching) and may be further specified as outlined in Table 3 and Figure S11. Irregular branching vessels may be defined as abnormal tortuous vessels, irregular caliber vessels, a lack of hierarchy in branching with varying branching angles, vessel sprouts or an overall impression of a chaotic vessel pattern. The term circumferential vessels relates to vessels that surround a lesion, whereas vessels located inside a lesion are called intralesional.

In the context of research, color flow within a lesion may be quantified using 3D ultrasound with virtual organ computer-aided analysis (VOCAL$^{TM}$) in order to calculate 3D power Doppler indices: the vascularity index (VI, the number of color voxels in the volume expressed as a percentage of the total number of voxels in the volume, potentially reflecting vascularity); the flow index (FI, the mean color value in the color voxels expressed as a number from 0–100, potentially reflecting flow velocity; and the vascularization flow index (VFI, calculated as VI multiplied by FI, reflecting the mean color value in all the volumes' voxels, expressed as a number from 0–100, and potentially reflecting tissue perfusion)[18,19]. However, because 3D vascular indices depend on machine settings, there remains doubt about their reproducibility, and their clinical use has yet to be explored adequately[19]. Until the limitations of these indices have been resolved, we recommend not using them outside the context of a specific research project.

 

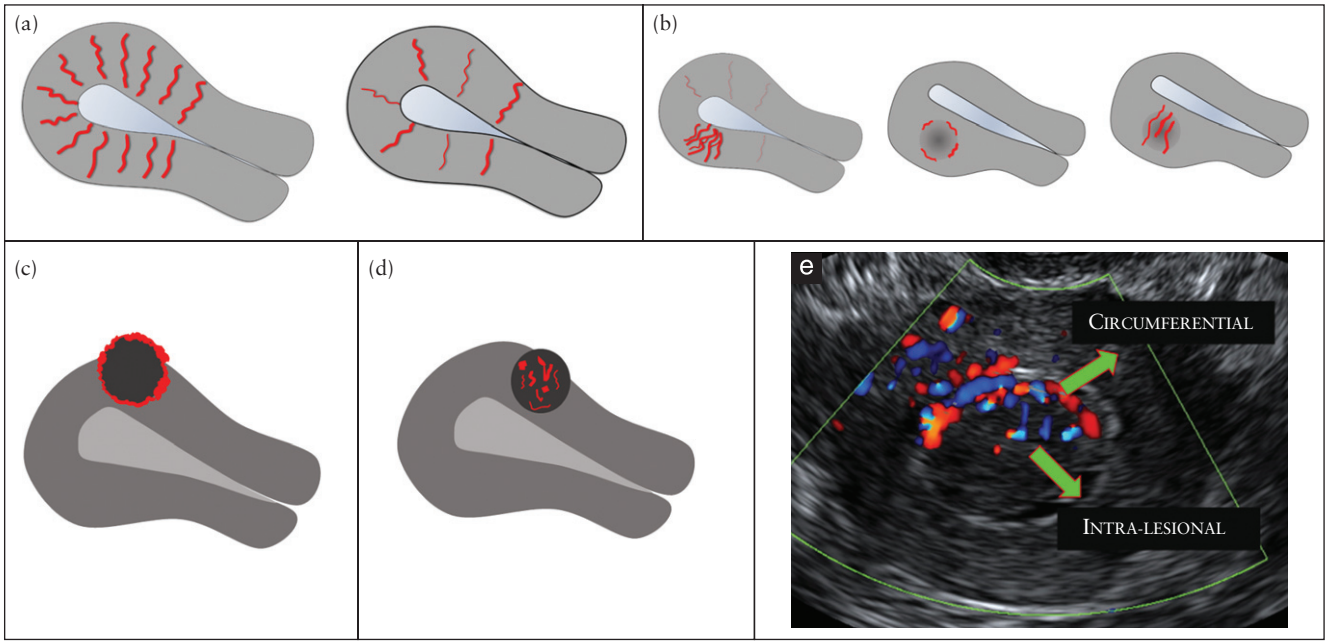


**Figure 8** Schematic and ultrasound images illustrating the vascular pattern within the myometrium and in myometrial lesions. The vascular pattern of the myometrium may be uniform (a) or non-uniform (b). The vascular pattern of a myometrial lesion may be circumferential (c), intralesional (d) or both (e).

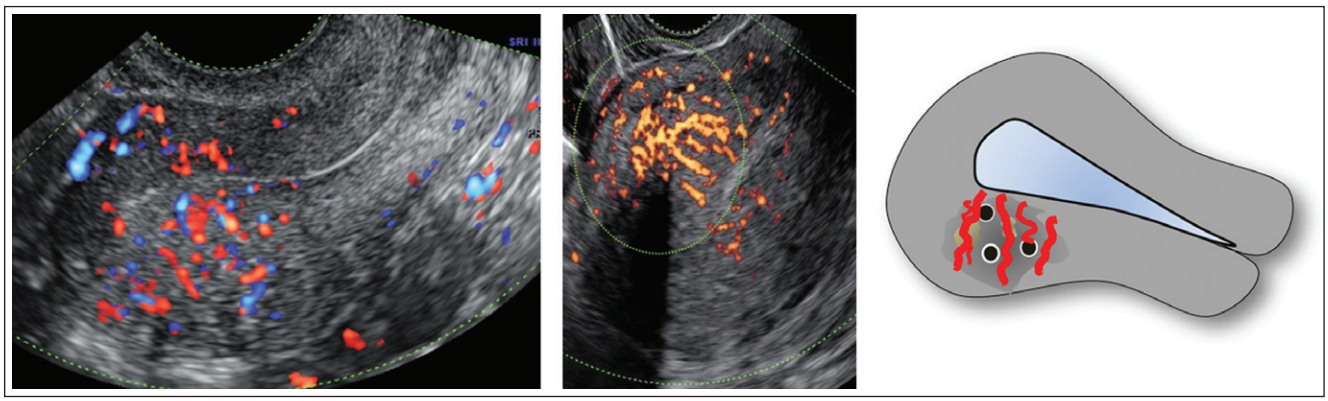

**Figure 9** Ultrasound images and schematic drawing illustrating translesional vascularity, defined as vessels perpendicular to the endometrium crossing the lesion.

## Examination of the myometrium in general clinical practice

In general clinical practice compared with a research setting, reporting on the myometrium may be more succinct (Table 4). The uterine corpus is measured, the symmetry of the myometrial walls is estimated and the overall echogenicity of the myometrium is reported as homogeneous or heterogeneous. If a myometrial lesion is observed, it is specified as well-defined or ill-defined. The number (or estimated number if there are more than four lesions) of lesions is reported, as well as the location, site and maximum diameter of the clinically relevant lesion(s). The presence of shadowing, myometrial cysts, hyperechogenic islands or subendometrial echogenic lines and buds is reported. The JZ is reported as regular or poorly defined (if it is irregular, interrupted, not visible or not assessable). When it is clinically relevant to evaluate vascularity, the overall vessel pattern within the myometrium of the whole uterus is reported as uniform or non-uniform. The amount of color within a lesion is reported using the color score (1 = no color; 2 = minimal color; 3 = moderate color; 4 = abundant color).

We propose inclusion of the following ultrasound images when reporting on the myometrium (ultrasound images of the endometrium should be described using IETA terminology[3]): at least one midsagittal section of the uterus (gray-scale and with power Doppler); preferably also a transverse section and/or coronal 3D reconstruction of the uterus; if a lesion is seen, at least one section of the uterus including the lesion; preferably also a detailed (zoomed) image of the lesion (in gray-scale and with power Doppler); for mapping of fibroids, 3D imaging showing the three standard orthogonal planes through the uterus or tomographic ultrasound images (TUI) may sometimes be illustrative.

 

**Table 3** Reporting vascularity of the myometrium on ultrasound examination

| *Vascularization to be assessed* | *Description* | *Measurement* |
|---|---|---|
| Whole uterus | | |
| Overall vessel pattern* (Figure 8) | Uniform, non-uniform* | — |
| Lesions | | |
| Amount of color (in a lesion)* (Figure S10) | Color score (both percentage of lesion being vascularized and color hue are taken into account)* | No color (1); minimal color (2); moderate color (3); abundant color (4)* |
| In case of uneven spread of vascularization† | Color score in most vascularized part† | No color (1); minimal color (2); moderate color (3); abundant color (4)† |
| | Percent of solid tissue with color signal† | 0–100%† |
| | Compared to adjacent myometrium† | Iso-, hypo-, hypervascularity† |
| Location of vessels† (Figures 8 and 9) | Circumferential, intralesional; uniform, non-uniform (areas with increased/decreased vascularity)† | — |
| Vessel morphology† (Figures 8 and S11) | Number: single, multiple; size: large and equal, small and equal, unequal; branching: regular, irregular, no branching; direction: perpendicular, not perpendicular† | — |

*Items of importance in daily clinical practice. †Items of interest for research purposes.

**Table 4** Reporting the myometrium in general clinical practice

| *Feature to be described* | *Description/term* |
|---|---|
| Uterine corpus | Length, anteroposterior diameter, transverse diameter |
| Myometrial walls | Symmetrical/asymmetrical |
| Overall echogenicity | Homogeneous/heterogeneous |
| Myometrial lesions | Well-defined/ill-defined |
| Number | Number (1, 2, 3 or estimation in case > 4 lesions) |
| Location | Location of the largest/clinically relevant lesion(s): anterior, posterior, fundal, right lateral or left lateral, global |
| Site | Site (for well-defined lesions) of the largest/clinically relevant lesion(s): FIGO classification 1–7 |
| Size | Maximum diameter of the largest/clinically relevant lesion(s) |
| Shadowing | |
| Edge shadows | Present/absent |
| Internal shadows | Present/absent |
| Fan-shaped shadowing | Present/absent |
| Cysts | Present/absent |
| Hyperechogenic islands | Present/absent |
| Subendometrial echogenic lines & buds | Present/absent |
| Junctional zone | Regular/poorly defined |
| Vascularity of myometrium | |
| Overall vessel pattern (in whole uterus) | Uniform/non-uniform |
| Amount of color (in a lesion): color score | (1) No color; (2) minimal color; (3) moderate color; (4) abundant color |

FIGO, International Federation of Gynecology and Obstetrics[2].

## ULTRASOUND FINDINGS ASSOCIATED WITH PATHOLOGY

In this section we describe ultrasound features that, in our opinion and on the basis of reports in the literature, are associated with pathology and in particular with adenomyosis and fibroids (Table 5). Further research should validate the importance of each of these features.

### Adenomyosis

Adenomyosis is caused by a proliferation of endometrial glands and stroma leading to ill-defined lesions within the myometrium. Adenomyosis may be present at one or more sites within the uterine wall or involve most of the myometrium, and may often be dispersed within the myometrium rather than forming a confined lesion, i.e. diffuse adenomyosis. It may, on the other hand, be present in only one part of the myometrium, i.e. focal adenomyosis. In rare cases it may present as a large cyst (an adenomyotic cyst or cystic adenomyoma)[20–24]. On histological examination, adenomyosis is classified as diffuse when the endometrial glands or stroma are distributed diffusely within the myometrium, and focal when circumscribed nodular aggregates are seen. Focal adenomyosis is not the same as an adenomyoma. These are defined by pathologists as focal adenomyosis with additional compensatory hypertrophy of the surrounding myometrium[25].

 

**Table 5** Features considered important in diagnosis of fibroids and adenomyosis

| *Feature* | *Typical fibroid* | *Adenomyosis* |
|---|---|---|
| Serosal contour of uterus | Lobulated or regular | Often globally enlarged uterus |
| Definition of lesion | Well-defined | Ill-defined in diffuse adenomyosis (adenomyoma may be well-defined) |
| Symmetry of uterine walls | Asymmetrical in presence of well-defined lesion(s) | Myometrial anteroposterior asymmetry |
| Lesion | | |
| Outline | Well-defined | Ill-defined |
| Shape | Round, oval, lobulated | Ill-defined |
| Contour | Smooth | Irregular or ill-defined |
| Rim | Hypo- or hyperechogenic | No rim |
| Shadowing | Edge shadows, internal shadows (often fan-shaped shadowing) | No edge shadows, fan-shaped shadowing[67] |
| Echogenicity | Uniform: hyper-, iso-, hypoechogenic<br>Non-uniform: mixed echogenicity | Non-uniform: mixed echogenicity[67,68]<br>Cysts[20–24,62], hyperechogenic islands, subendometrial lines and buds[24,63] |
| Vascularity | Circumferential flow | Translesional flow[69] |
| Junctional zone (JZ) | | |
| JZ thickness, regularity | Not-thickened; regular or not visible | Thickened; irregular or ill-defined[9,61–63] |
| JZ interruption | Interrupted or overstretched JZ in areas with lesions of FIGO types 1–3 (Figure 3) | Interrupted JZ (even in absence of localized lesions)[9] |

FIGO, International Federation of Gynecology and Obstetrics[2].

The ultrasound features of adenomyosis (Figure 10) should be reported and quantified (Tables 1–3). The ultrasound features of a globular uterus with ill-defined adenomyotic lesions may be explained by direct invasion of endometrial tissue from the endometrium, as seen in 'classic adenomyosis', or by invasion from endometriotic implants on the serosal surface of the uterus[26]. Rarely, diffuse adenomyosis may be localized as a solitary finding without direct continuation with the serosa or the endometrium[22]. The relative proportions of endometrial glandular structures, endometrial stroma and hypertrophic muscle elements within a lesion probably explain the different ultrasound features reported to be typical of adenomyosis. The link between ultrasound features and histopathology has yet to be confirmed and requires further research[27].

## Fibroid (leiomyoma)

A uterine fibroid is seen typically on ultrasound as a well-defined round lesion within the myometrium or attached to it, often showing shadows at the edge of the lesion and/or internal fan-shaped shadowing (Figure S12). The echogenicity varies and some hyperechogenicity may be present internally. On color- or power-Doppler imaging, circumferential flow around the lesion is often visible. However, some fibroids do not exhibit such typical features. We suggest that such fibroids are labelled as sonographically atypical fibroids (Figure 11).

On histological examination, fibroids are composed of smooth muscle cells and connective tissue in densely packed whorls. Acoustic shadowing may arise from the interface between smooth muscle bundles, hyalinized connective tissue and normal myometrium[28]. The sonographic appearance of a fibroid may depend on the proportion of muscle cells and fibrous stroma within the lesion.

## Variants of fibroids and other uterine smooth muscle tumors

### *Variants of fibroids*

Fibroids may undergo degeneration, which may be spontaneous or a result of induced infarction following uterine artery embolization. Coagulate necrosis is induced after high-intensity ultrasound or radiofrequency ablation. Types of degeneration are: a) red, b) hyaline, c) cystic/myxoid (myxoid leiomyoma) or d) hydropic. Spontaneous degeneration may occur in pregnancy, and red degeneration is an initial manifestation[29] within days after infarction. The sonographic appearance of red degeneration may be unremarkable, although some cases have been reported as homogeneous lesions with low echogenicity, a hyperechogenic rim and absent internal vascularity[30–32]. Hemorrhage and edema in these fibroids may give rise to tumors of mixed echogenicity. Late manifestations after infarction are most commonly hyaline degeneration[33,34], while some fibroids may show mixed echogenicity or hypoechogenic cystic areas.

Fibroids after induced infarction are often uniform, hypoechogenic with a hyperechogenic rim and acoustic shadows[35,36]. There is usually no internal vascularity or, at most, a few disparate vessels are observed. Cystic or myxoid degeneration may develop, resulting in regular hypoechogenic cystic areas with fluid or myxoid content[37,38]. Degeneration may also occur in malignant uterine smooth muscle tumors[39].

### *Uterine sarcomas and other uterine smooth-muscle tumors*

The prediction of malignancy is of utmost importance. However, data on the prediction of uterine sarcoma by ultrasound examination are scarce and based mainly

 

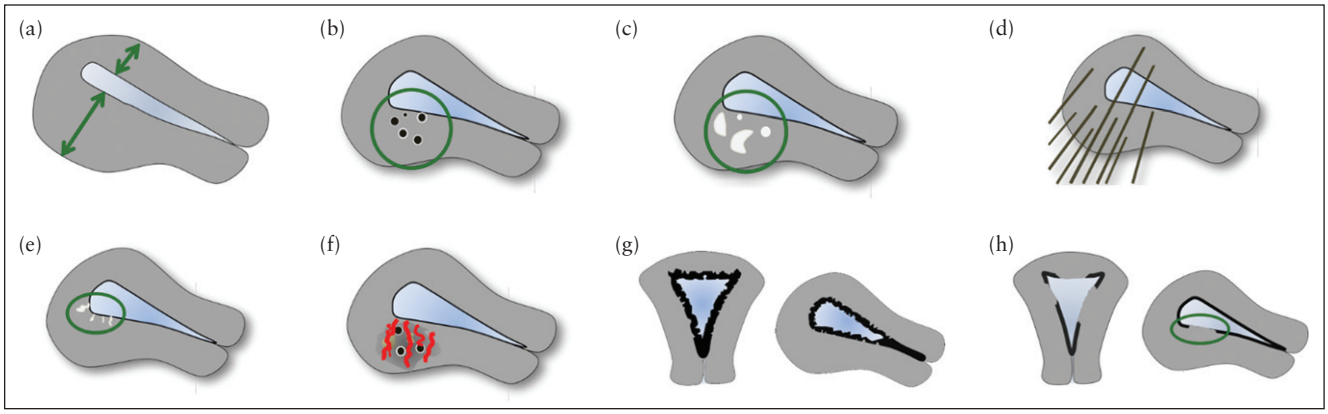


**Figure 10** Schematic drawings illustrating the ultrasound features considered currently to be typical of adenomyosis: asymmetrical thickening (a), cysts (b), hyperechoic islands (c), fan-shaped shadowing (d), echogenic subendometrial lines and buds (e), translesional vascularity (f), irregular junctional zone (g) and interrupted junctional zone (h).

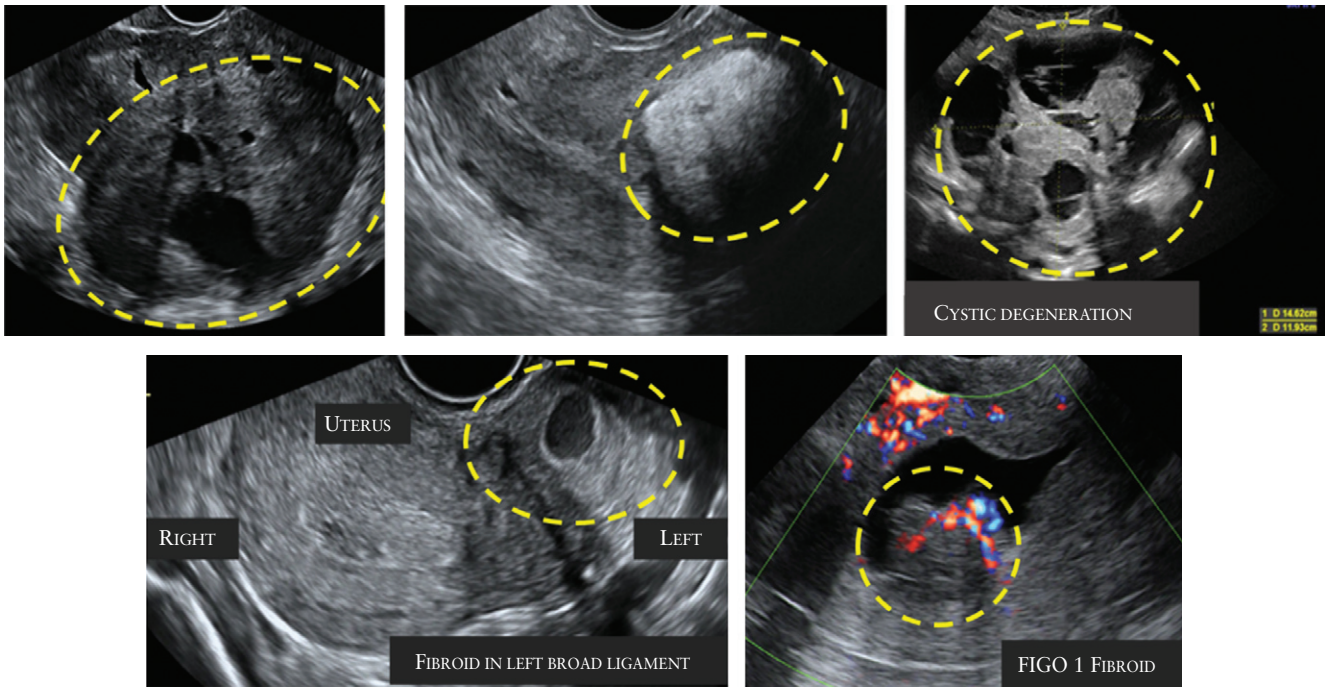


**Figure 11** Ultrasound images showing fibroids with atypical sonographic features. These fibroids have non-uniform echogenicity and intralesional anechoic cysts, and some have areas with hyperechogenicity. The FIGO type 1 fibroid (bottom right) has an irregular outline.

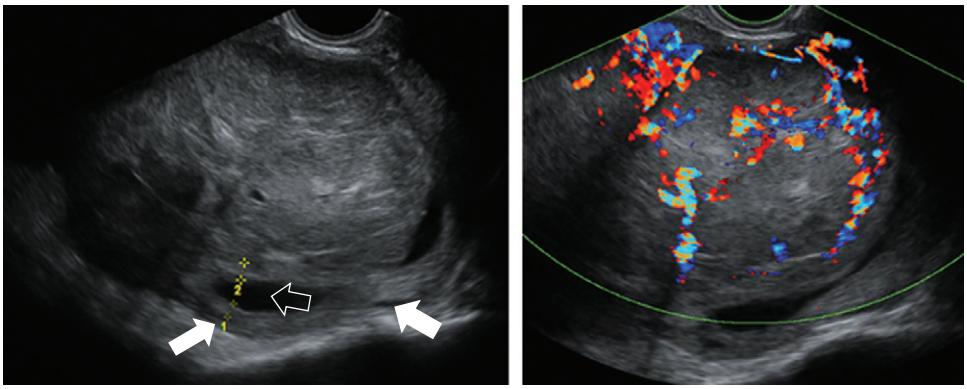

**Figure 12** Gray-scale and color Doppler images of a sarcoma in the anterior wall of the uterus. The uterine corpus (solid arrows) is located posteriorly and contains clear fluid (open arrow).

 

on small retrospective case series, precluding definitive guidelines. There are many rare uterine smooth-muscle tumors other than benign leiomyomas[40], but only limited information on their ultrasound features has been reported to date. This issue has become increasingly important in view of the debate about when, or if, fibroids may be morcellated during laparoscopic surgery.

Malignant sarcomas comprise leiomyosarcoma (Figure 12), endometrial stromal sarcoma, adenosarcoma and undifferentiated sarcoma. Uterine sarcomas present as purely myometrial lesions and are typically single, large tumors[41]. Their ultrasound features may be indistinct from those of ordinary fibroids[42] or they may appear as an irregularly vascularized mass, with a regular or irregular outline, often with irregular anechoic areas due to necrosis[43–49].

### *Uterine smooth-muscle tumor of uncertain malignant potential (STUMP)*

There are no specific ultrasound features described for STUMP. Intravenous leiomyomatosis, disseminated peritoneal leiomyomatosis and benign metastasizing leiomyoma[50–52] have the same ultrasound features as do ordinary fibroids. There are often multiple fibroids and they may be recognized by their location outside the uterine borders. These multiple fibroids should be distinguished from diffuse leiomyomatosis[53].

### *Fibroids with little or no recurrent and/or metastatic potential*

Ultrasound features of leiomyoma with bizarre nuclei (bizarre/symplastic/atypical leiomyoma), mitotically active leiomyoma, cellular and highly cellular leiomyoma, dissecting leiomyoma and leiomyoma with increased cellularity, no atypia or mitotic figures and increased vascularity[40,54] may have the same macroscopically pathological features as do fibroids[40,54] and may have increased vascularity, as this feature seems to be related to cellularity[55]. A cotyledonoid leiomyoma or cotelydonoid dissecting leiomyoma[56–58] is a nodular tumor with placenta-like echogenicity on ultrasound, but may also be cystic. Ultrasonographic features of lipoleiomyoma[59] comprise a hyperechogenic mass partly encased by a hypoechogenic rim. Ultrasonographic features for epithelioid leiomyoma[40] and palisading/neurilemmoma-like leiomyoma[60] have not been described.

## CONCLUSION

The terms and definitions presented in this paper aim to facilitate consistent reporting of myometrial lesions when using ultrasonography in both daily clinical practice and for research purposes. Clearly, the clinical relevance of some of the terms that have been proposed has not yet been evaluated in prospective clinical studies. We acknowledge that some aspects of the systematic reporting we have suggested may require a relatively high level of ultrasound training. We also acknowledge that some of the proposed terms and definitions are too detailed for use in general clinical practice and will initially be suitable only for use in research settings. Future research should focus on the ability to predict specific pathologies and on the clinical relevance of the ultrasound features described in this paper. Although the members of the panel involved in the writing of this consensus have different fields of expertise, including gynecological ultrasonography, fertility treatment, hysteroscopy, general gynecology and clinical research, we acknowledge that they all come from Europe and the USA, leaving most areas of the world unrepresented.

The recent controversy about the safety of morcellation of lesions thought to be benign fibroids, but that were in fact malignant[5], highlights the importance of reliable preoperative characterization of myometrial lesions. Although recognizing a typical fibroid on ultrasound is usually straightforward, differentiating between an atypical fibroid and a uterine sarcoma remains challenging. The establishment of an international database of ultrasound imaging and magnetic resonance imaging (MRI) of uterine sarcomas and rare uterine tumors would be of great clinical value.

Adenomyosis may be difficult to diagnose with ultrasound. Different ultrasound features have been suggested to be associated with adenomyosis, but at present it is not clear which of the various ultrasound criteria are most important for diagnosis. Some features may carry a greater diagnostic weight than others[61] and the presence of more than one ultrasound feature associated with adenomyosis might increase the likelihood of the diagnosis[61–63]. We have not included in our consensus statement the so called 'question-mark sign', suggested to be typical of adenomyosis, because this sign occurs when there is also deep infiltrating endometriosis in the posterior compartment[64].

The terms that we suggest for characterization of the JZ are derived from MRI studies[20,30]. The JZ is better visualized by 3D[9,65] than by 2D ultrasound, but the clinical implications of a thickened or disrupted JZ on ultrasound needs to be established[4,66].

The clinical relevance of myometrial lesions for abnormal uterine bleeding, pelvic pain, subfertility and pregnancy outcome is an important topic for research. Certain ultrasound features might prove to be more clinically relevant than others. The role of a systematic evaluation of the sonographic features of myometrial lesions when choosing management (expectant management, medical therapy, selective embolization, high-intensity focused ultrasound or surgical treatment) and in the follow-up during or after treatment is another important topic for future research.

To conclude, the terms and definitions in this consensus statement should enable clinicians to produce a structured report when describing the sonographic appearance of the myometrium and myometrial lesions and harmonize nomenclature for future research.

 

## ACKNOWLEDGMENTS

T.B. is supported by the National Institute for Health Research (NIHR) Biomedical Research Centre based at Imperial College Healthcare NHS Trust and Imperial College London. The views expressed are those of the author(s) and not necessarily those of the NHS, the NIHR or the Department of Health. D.T. is Senior Clinical Investigator of Scientific Research Fund (FWO) Flanders.

## REFERENCES

1. Munro MG, Critchley HO, Fraser IS. The FIGO classification of causes of abnormal uterine bleeding in the reproductive years. *Fertil Steril* 2011; **95**: 2204–2208.
2. Munro MG, Critchley HO, Broder MS, Fraser IS. FIGO classification system (PALM-COEIN) for causes of abnormal uterine bleeding in nongravid women of reproductive age. *Int J Gynaecol Obstet* 2011; **113**: 3–13.
3. Leone FP, Timmerman D, Bourne T, Valentin L, Epstein E, Goldstein SR, Marret H, Parsons AK, Gull B, Istre O, Sepulveda W, Ferrazzi E, Van den Bosch T. Terms, definitions and measurements to describe the sonographic features of the endometrium and intrauterine lesions: a consensus opinion from the International Endometrial Tumor Analysis (IETA) group. *Ultrasound Obstet Gynecol* 2010; **35**: 103–112.
4. Gordts S, Brosens JJ, Fusi L, Benagiano G, Brosens I. Uterine adenomyosis: a need for uniform terminology and consensus classification. *Reprod Biomed Online* 2008; **17**: 244–248.
5. Hampton T. Critics of fibroid removal procedure question risks it may pose for women with undetected uterine cancer. *JAMA* 2014; **311**: 891–893.
6. Okaro E, Condous G, Khalid A, Timmerman D, Ameye L, Van Huffel SV, Bourne T. The use of ultrasound-based 'soft markers' for the prediction of pelvic pathology in women with chronic pelvic pain--can we reduce the need for laparoscopy? *BJOG* 2006; **113**: 251–256.
7. Tetlow RL, Richmond I, Manton DJ, Greenman J, Turnbull LW, Killick SR. Histological analysis of the uterine junctional zone as seen by transvaginal ultrasound. *Ultrasound Obstet Gynecol* 1999; **14**: 188–193.
8. Naftalin J, Jurkovic D. The endometrial-myometrial junction: a fresh look at a busy crossing. *Ultrasound Obstet Gynecol* 2009; **34**: 1–11.
9. Exacoustos C, Brienza L, Di GA, Szabolcs B, Romanini ME, Zupi E, Arduini D. Adenomyosis: three-dimensional sonographic findings of the junctional zone and correlation with histology. *Ultrasound Obstet Gynecol* 2011; **37**: 471–479.
10. Exacoustos C, Luciano D, Corbett B, De FG, Di FM, Luciano A, Zupi E. The uterine junctional zone: a 3-dimensional ultrasound study of patients with endometriosis. *Am J Obstet Gynecol* 2013; **209**: 248.e1–7.
11. Martins WP, Raine-Fenning NJ, Leite SP, Ferriani RA, Nastri CO. A standardized measurement technique may improve the reliability of measurements of endometrial thickness and volume. *Ultrasound Obstet Gynecol* 2011; **38**: 107–115.
12. Woelfer B, Salim R, Banerjee S, Elson J, Regan L, Jurkovic D. Reproductive outcomes in women with congenital uterine anomalies detected by three-dimensional ultrasound screening. *Obstet Gynecol* 2001; **98**: 1099–1103.
13. Abuhamad AZ, Singleton S, Zhao Y, Bocca S. The Z technique: an easy approach to the display of the mid-coronal plane of the uterus in volume sonography. *J Ultrasound Med* 2006; **25**: 607–612.
14. Wamsteker K, Emanuel MH, de Kruif JH. Transcervical hysteroscopic resection of submucous fibroids for abnormal uterine bleeding: results regarding the degree of intramural extension. *Obstet Gynecol* 1993; **82**: 736–740.
15. Casadio P, Youssef AM, Spagnolo E, Rizzo MA, Talamo MR, De AD, Marra E, Ghi T, Savelli L, Farina A, Pelusi G, Mazzon I. Should the myometrial free margin still be considered a limiting factor for hysteroscopic resection of submucous fibroids? A possible answer to an old question. *Fertil Steril* 2011; **95**: 1764–1768.
16. Yang JH, Lin BL. Changes in myometrial thickness during hysteroscopic resection of deeply invasive submucous myomas. *J Am Assoc Gynecol Laparosc* 2001; **8**: 501–505.
17. Timmerman D, Valentin L, Bourne TH, Collins WP, Verrelst H, Vergote I. Terms, definitions and measurements to describe the sonographic features of adnexal tumors: a consensus opinion from the International Ovarian Tumor Analysis (IOTA) Group. *Ultrasound Obstet Gynecol* 2000; **16**: 500–505.
18. Alcazar JL. Three-dimensional power Doppler derived vascular indices: what are we measuring and how are we doing it? *Ultrasound Obstet Gynecol* 2008; **32**: 485–487.
19. Raine-Fenning NJ, Campbell BK, Clewes JS, Kendall NR, Johnson IR. The reliability of virtual organ computer-aided analysis (VOCAL) for the semiquantification of ovarian, endometrial and subendometrial perfusion. *Ultrasound Obstet Gynecol* 2003; **22**: 633–639.
20. Cucinella G, Billone V, Pitruzzella I, Lo Monte AI, Palumbo VD, Perino A. Adenomyotic cyst in a 25-year-old woman: case report. *J Minim Invasive Gynecol* 2013; **20**: 894–898.
21. Ho ML, Ratts V, Merritt D. Adenomyotic cyst in an adolescent girl. *J Pediatr Adolesc Gynecol* 2009; **22**: 33–38.
22. Protopapas A, Milingos S, Markaki S, Loutradis D, Haidopoulos D, Sotiropoulou M, Antsaklis A. Cystic uterine tumors. *Gynecol Obstet Invest* 2008; **65**: 275–280.
23. Tahlan A, Nanda A, Mohan H. Uterine adenomyoma: a clinicopathologic review of 26 cases and a review of the literature. *Int J Gynecol Pathol* 2006; **25**: 361–365.
24. Reinhold C, Tafazoli F, Mehio A, Wang L, Atri M, Siegelman ES, Rohoman L. Uterine adenomyosis: endovaginal US and MR imaging features with histopathologic correlation. *Radiographics* 1999; **19**: 147–160.
25. Haines, Taylor. Obstetrical and Gynaecological Pathology. (4th edn), Fox H, Wells M (eds). Churchill Livingstone, 1995.
26. Kishi Y, Suginami H, Kuramori R, Yabuta M, Suginami R, Taniguchi F. Four subtypes of adenomyosis assessed by magnetic resonance imaging and their specification. *Am J Obstet Gynecol* 2012; **207**: 114–117.
27. Ferenczy A. Pathophysiology of adenomyosis. *Hum Reprod Update* 1998; **4**: 312–322.
28. Kliewer MA, Hertzberg BS, George PY, McDonald JW, Bowie JD, Carroll BA. Acoustic shadowing from uterine leiomyomas: sonographic-pathologic correlation. *Radiology* 1995; **196**: 99–102.
29. Ouyang DW, Economy KE, Norwitz ER. Obstetric complications of fibroids. *Obstet Gynecol Clin North Am* 2006; **33**: 153–169.
30. Lev-Toaff AS, Coleman BG, Arger PH, Mintz MC, Arenson RL, Toaff ME. Leiomyomas in pregnancy: sonographic study. *Radiology* 1987; **164**: 375–380.
31. Cooper NP, Okolo S. Fibroids in pregnancy--common but poorly understood. *Obstet Gynecol Surv* 2005; **60**: 132–138.
32. Valentin L. Characterising acute gynaecological pathology with ultrasound: an overview and case examples. *Best Pract Res Clin Obstet Gynaecol* 2009; **23**: 577–593.
33. McLucas B. Diagnosis, imaging and anatomical classification of uterine fibroids. *Best Pract Res Clin Obstet Gynaecol* 2008; **22**: 627–642.
34. Ueda H, Togashi K, Konishi I, Kataoka ML, Koyama T, Fujiwara T, Kobayashi H, Fujii S, Konishi J. Unusual appearances of uterine leiomyomas: MR imaging findings and their histopathologic backgrounds. *Radiographics* 1999; **19**: 131–145.
35. Nicholson TA, Pelage JP, Ettles DF. Fibroid calcification after uterine artery embolization: ultrasonographic appearance and pathology. *J Vasc Interv Radiol* 2001; **12**: 443–446.
36. Allison SJ, Wolfman DJ. Sonographic evaluation of patients treated with uterine artery embolization. *Ultrasound Clinics* 2010; **5**: 277–288.
37. Yarwood RL, Arroyo E. Cystic degeneration of a uterine leiomyoma masquerading as a postmenopausal ovarian cyst. A case report. *J Reprod Med* 1999; **44**: 649–652.
38. Cohen JR, Luxman D, Sagi J, Jossiphov J, David MP. Ultrasonic "honeycomb" appearance of uterine submucous fibroids undergoing cystic degeneration. *J Clin Ultrasound* 1995; **23**: 293–296.
39. Karpathiou G, Sivridis E, Giatromanolaki A. Myxoid leiomyosarcoma of the uterus: a diagnostic challenge. *Eur J Gynaecol Oncol* 2010; **31**: 446–448.
40. Ip PP, Tse KY, Tam KF. Uterine smooth muscle tumors other than the ordinary leiomyomas and leiomyosarcomas: a review of selected variants with emphasis on recent advances and unusual morphology that may cause concern for malignancy. *Adv Anat Pathol* 2010; **17**: 91–112.
41. Bonneau C, Thomassin-Naggara I, Dechoux S, Cortez A, Darai E, Rouzier R. Value of ultrasonography and magnetic resonance imaging for the characterization of uterine mesenchymal tumors. *Acta Obstet Gynecol Scand* 2013; **93**: 261–268.
42. Jayakrishnan K, Koshy AK, Manjula P, Nair AM, Ramachandran A, Kattoor J. Endometrial stromal sarcoma mimicking a myoma. *Fertil Steril* 2009; **92**: 1744–1746.
43. Exacoustos C, Romanini ME, Amadio A, Amoroso C, Szabolcs B, Zupi E, Arduini D. Can gray-scale and color Doppler sonography differentiate between uterine leiomyosarcoma and leiomyoma? *J Clin Ultrasound* 2007; **35**: 449–457.
44. Aviram R, Ochshorn Y, Markovitch O, Fishman A, Cohen I, Altaras MM, Tepper R. Uterine sarcomas versus leiomyomas: gray-scale and Doppler sonographic findings. *J Clin Ultrasound* 2005; **33**: 10–13.
45. Hata K, Hata T, Maruyama R, Hirai M. Uterine sarcoma: can it be differentiated from uterine leiomyoma with Doppler ultrasonography? A preliminary report. *Ultrasound Obstet Gynecol* 1997; **9**: 101–104.
46. Seki K, Hoshihara T, Nagata I. Leiomyosarcoma of the uterus: ultrasonography and serum lactate dehydrogenase level. *Gynecol Obstet Invest* 1992; **33**: 114–118.
47. Hata K, Hata T, Makihara K, Aoki S, Takamiya O, Kitao M, Harada Y, Nagaoka S. Sonographic findings of uterine leiomyosarcoma. *Gynecol Obstet Invest* 1990; **30**: 242–245.
48. Szabo I, Szantho A, Csabay L, Csapo Z, Szirmai K, Papp Z. Color Doppler ultrasonography in the differentiation of uterine sarcomas from uterine leiomyomas. *Eur J Gynaecol Oncol* 2002; **23**: 29–34.
49. Amant F, Coosemans A, Debiec-Rychter M, Timmerman D, Vergote I. Clinical management of uterine sarcomas. *Lancet Oncol* 2009; **10**: 1188–1198.
50. Fasih N, Prasad Shanbhogue AK, Macdonald DB, Fraser-Hill MA, Papadatos D, Kielar AZ, Doherty GP, Walsh C, McInnes M, Atri M. Leiomyomas beyond the uterus: unusual locations, rare manifestations. *Radiographics* 2008; **28**: 1931–1948.
51. Cohen DT, Oliva E, Hahn PF, Fuller AF, Jr., Lee SI. Uterine smooth-muscle tumors with unusual growth patterns: imaging with pathologic correlation. *AJR Am J Roentgenol* 2007; **188**: 246–255.
52. Vaquero ME, Magrina JF, Leslie KO. Uterine smooth-muscle tumors with unusual growth patterns. *J Minim Invasive Gynecol* 2009; **16**: 263–268.
53. Fedele L, Bianchi S, Zanconato G, Carinelli S, Berlanda N. Conservative treatment of diffuse uterine leiomyomatosis. *Fertil Steril* 2004; **82**: 450–453.
54. Robboy SJ, Bentley RC, Butnor K, Anderson MC. Pathology and pathophysiology of uterine smooth-muscle tumors. *Environ Health Perspect* 2000; **108** Suppl 5: 779–784.
55. Minsart AF, Ntoutoume SF, Vandenhoute K, Jani J, Van PC. Does three-dimensional power Doppler ultrasound predict histopathological findings of uterine fibroids? A preliminary study. *Ultrasound Obstet Gynecol* 2012; **40**: 714–720.
56. Smith CC, Gold MA, Wile G, Fadare O. Cotyledonoid dissecting leiomyoma of the uterus: a review of clinical, pathological, and radiological features. *Int J Surg Pathol* 2012; **20**: 330–341.

 

57. Raga F, Sanz-Cortes M, Casan EM, Burgues O, Bonilla-Musoles F. Cotyledonoid dissecting leiomyoma of the uterus. *Fertil Steril* 2009; **91**: 1269–1270.
58. Gurbuz A, Karateke A, Kabaca C, Arik H, Bilgic R. A case of cotyledonoid leiomyoma and review of the literature. *Int J Gynecol Cancer* 2005; **15**: 1218–1221.
59. Prieto A, Crespo C, Pardo A, Docal I, Calzada J, Alonso P. Uterine lipoleiomyomas: US and CT findings. *Abdom Imaging* 2000; **25**: 655–657.
60. Gisser SD, Young I. Neurilemoma-like uterine myomas:an ultrastructural reaffirmation of their non-Schwannian nature. *Am J Obstet Gynecol* 1977; **129**: 389–392.
61. Dueholm M, Lundorf E, Hansen ES, Sorensen JS, Ledertoug S, Olesen F. Magnetic resonance imaging and transvaginal ultrasonography for the diagnosis of adenomyosis. *Fertil Steril* 2001; **76**: 588–594.
62. Bazot M, Cortez A, Darai E, Rouger J, Chopier J, Antoine JM, Uzan S. Ultrasonography compared with magnetic resonance imaging for the diagnosis of adenomyosis: correlation with histopathology. *Hum Reprod* 2001; **16**: 2427–2433.
63. Kepkep K, Tuncay YA, Goynumer G, Tutal E. Transvaginal sonography in the diagnosis of adenomyosis: which findings are most accurate? *Ultrasound Obstet Gynecol* 2007; **30**: 341–345.
64. Di Donato N, Bertoldo V, Montanari G, Zannoni L, Caprara G, Seracchioli R. Question mark form of uterus: a simple sonographic sign associated with the presence of adenomyosis. *Ultrasound Obstet Gynecol* 2015; **46**: 126–127.
65. Naftalin J, Hoo W, Nunes N, Mavrelos D, Nicks H, Jurkovic D. Inter- and intraobserver variability in three-dimensional ultrasound assessment of the endometrial-myometrial junction and factors affecting its visualization. *Ultrasound Obstet Gynecol* 2012; **39**: 587–591.
66. Tocci A, Greco E, Ubaldi FM. Adenomyosis and 'endometrial-subendometrial myometrium unit disruption disease' are two different entities. *Reprod Biomed Online* 2008; **17**: 281–291.
67. Dueholm M. Transvaginal ultrasound for diagnosis of adenomyosis: a review. *Best Pract Res Clin Obstet Gynaecol* 2006; **20**: 569–582.
68. Reinhold C, Tafazoli F, Wang L. Imaging features of adenomyosis. *Hum Reprod Update* 1998; **4**: 337–349.
69. Chiang CH, Chang MY, Hsu JJ, Chiu TH, Lee KF, Hsieh TT, Soong YK. Tumor vascular pattern and blood flow impedance in the differential diagnosis of leiomyoma and adenomyosis by color Doppler sonography. *J Assist Reprod Genet* 1999; **16**: 268–275.


## SUPPORTING INFORMATION ON THE INTERNET

The following supporting information may be found in the online version of this article:

**Figure S1** Schematic drawings illustrating how to measure the uterus.

**Figure S2** Schematic drawings illustrating how to describe the serosal contour of the uterus.

**Figure S3** Schematic drawings illustrating symmetry of the uterine walls.

**Figure S4** Schematic drawings and ultrasound images illustrating measurement of the junctional zone thickness (for research purposes).

**Figure S5** Schematic drawings illustrating measurement of the inner lesion-free margin and outer lesion-free margin of a lesion.

**Figure S6** Measurement of lesion penetration (for research purposes).

**Figure S7** Schematic drawings illustrating echogenicity of a uniform lesion (for research purposes).

**Figure S8** Schematic drawings illustrating the rim and shape of myometrial lesions.

**Figure S9** Schematic and ultrasound images illustrating the normal vascular pattern of the myometrium.

**Figure S10** Schematic images illustrating the color score (amount of color Doppler signals) in the circumference of and inside myometrial lesions.

**Figure S11** Schematic drawings illustrating how to describe the vascularization of a myometrial lesion in clinical research.

**Figure S12** Schematic drawings illustrating the ultrasound features considered currently to be typical of uterine fibroids.

 